Supplement of

Potential modulation of Indian Ocean basin mode on the interdecadal variations of summer precipitation over the East Asian monsoon boundary zone

Jing Wang et al.

Correspondence: Yanju Liu (liuyanj@cma.gov.cn)

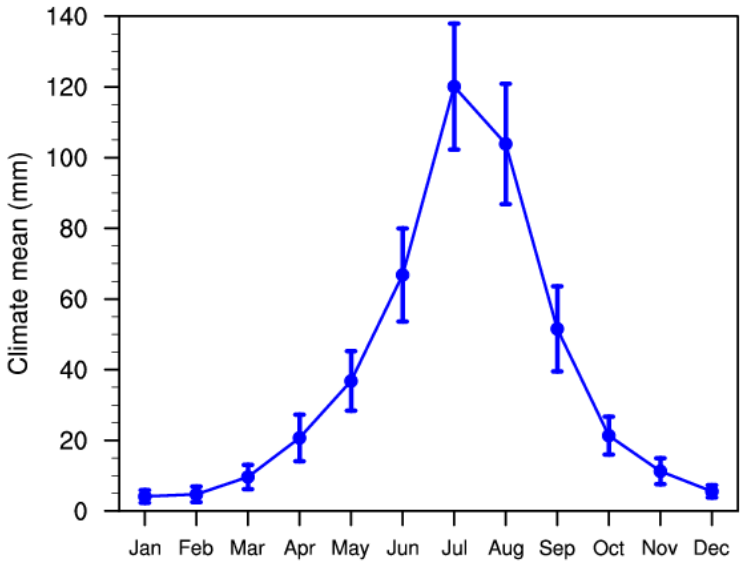

Figure S1. Annual cycle of the climatological-mean (1901–2014) EAMBZ precipitation (mm). The error bars denote one standard deviation from the mean. The precipitation is derived from the CRU TS3.26 precipitation data.

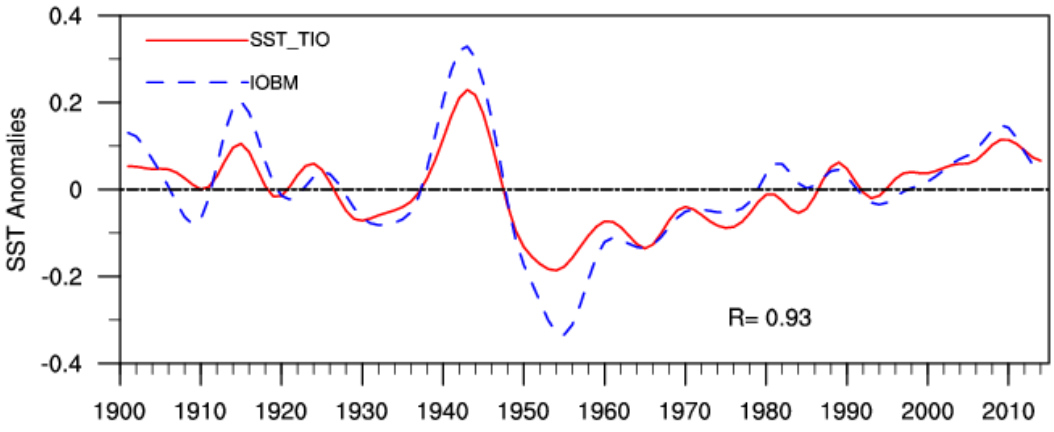

Figure S2. Time-evolving observed summertime SSTAs over the narrower TIO domain for defining I_{IOBM} (20 °S–20 °N, 40 °–100 °E; blue line) and SSTAs over the broader TIO domain in CESM1_IOPES (15 °S–15 °N, 40 °–174 °E; red line) from 1901–2014. The time series are detrended and 11-year low-pass filtered. The numeral at the bottom represents the TCC between the corresponding time series. The base period for calculating SSTAs is 1901–2014. The areal mean SSTAs are calculated based on the ERSSTv5.

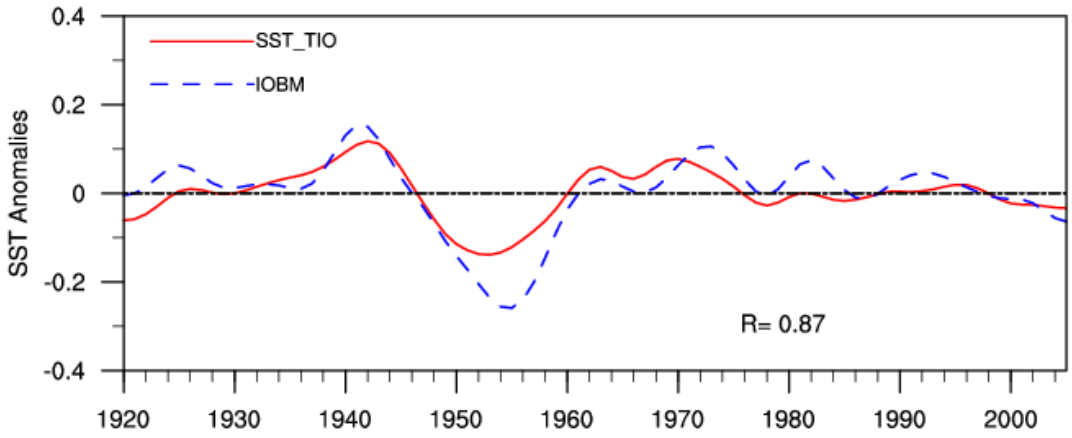

Figure S3. Time-evolving simulated summertime SSTAs over the narrower TIO domain for defining I_{IOBM} (20 °S–20 °N, 40 °–100 °E; blue line) and SSTAs over the broader TIO domain in CESM1_IOPES (15 °S–15 °N, 40 °–174 °E; red line) from 1920–2005. The time series are detrended and 11-year low-pass filtered. The numeral at the bottom represents the TCC between the corresponding time series. The areal mean SSTAs are calculated based on the difference between the CESM1_IOPES ensemble mean and the CESM1_LENS ensemble mean (former minus latter).

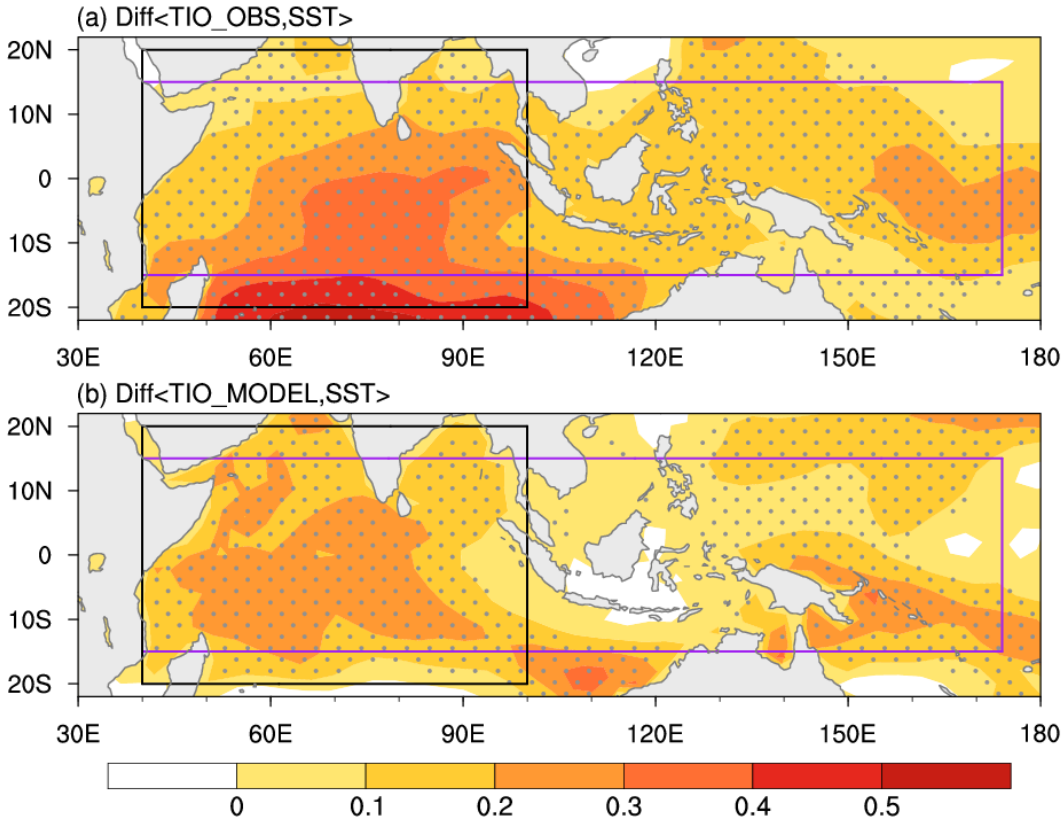

Figure S4. Composite differences of (a) observed and (b) simulated JJA-mean SST (℃) between warm and cold SST years over the broader TIO domain in CESM1_IOPES (15 ℃S–15 ℃N, 40 °–174 ℃E; purple box). In panel (a), the warm and cold TIO SST years are selected based on the ±0.5 standard deviations of the observed time-evolving SSTAs during 1901–2014, as shown in Fig. S2 (red line). In panel (b), the warm and cold TIO SST years are selected based on the ±0.5 standard deviations of the simulated time-evolving SSTAs during 1920–2005, as shown in Fig. S3 (red line). The black frame (20 ℃S–20 ℃N, 40 °–100 ℃E) outlines the domain for delineating the IOBM mode (the same hereinafter). All variables are detrended and 11-year low-pass filtered. Areas with significant values exceeding the 95% confidence level are dotted. The observed SSTAs are derived from the ERSSTv5; whilst the simulated SSTAs are calculated based on the difference between the CESM1_IOPES ensemble mean and the CESM1_LENS ensemble mean (former minus latter), highlighting the internally driven impacts of TIO SSTAs.

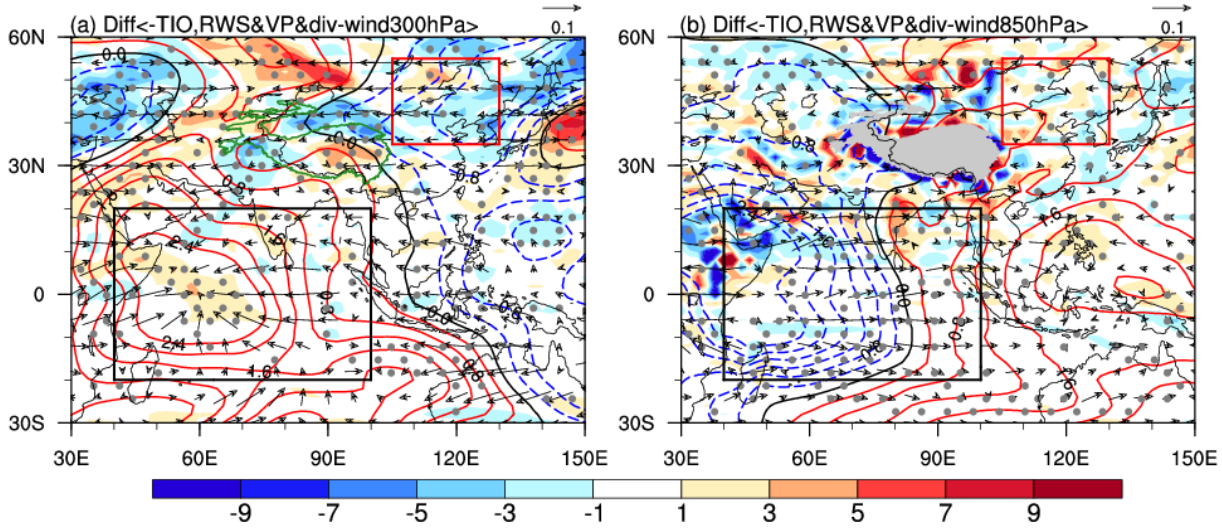

153

154 **Figure S5.** Simulated composite differences of JJA-mean (a) 300- and (b) 850-hPa RWS (shading; 10^{-11} s^{-2}),
155 velocity potential (contours; interval: 0.8; 10^5 m^2 s^{-1}), and divergent horizontal wind (vectors; m s^{-1}) between cold
156 and warm SST years over the broader TIO domain in CESM1_IOPES (15 °S–15 °N, 40 °–174 °E; purple box in Fig.
157 S4). The warm and cold TIO SST years are selected based on the ±0.5 standard deviations of the simulated
158 time-evolving SSTAs during 1920–2005, as shown in Fig. S3 (red line). All variables are detrended and 11-year
159 low-pass filtered. Areas with significant values of RWS exceeding the 95% confidence level are stippled. Only
160 vectors that are significant at the 95% confidence level are shown. The simulated anomalies of RWS, velocity
161 potential, and divergent horizontal wind are calculated based on the difference between the CESM1_IOPES
162 ensemble mean and the CESM1_LENS ensemble mean (former minus latter), highlighting the internally driven
163 impacts of TIO SSTAs.

164

165

166

167

168

169